Develop. Growth Differ. (2009) **51**, 443–451 doi: 10.1111/j.1440-169X.2009.01107.x

Original Article

Developmental expression of *Xenopus* myosin 1d and identification of a myo1d tail homology that overlaps TH1

Janine M. LeBlanc-Straceski,[1]* Anna Sokac,[2] William Bement,[2] Pablo Sobrado[1,3] and Laura Lemoine[1,4]

[1]*Department of Biology, Merrimack College, 315 Turnpike Street, North Andover, Massachusetts 01845;* [2]*Department of Zoology, University of Wisconsin, Madison, Wisconsin;* [3]*Department of Biochemistry, Virginia Polytechnic Institute and State University, Blacksburg, Virginia;* [4]*Program in Molecular Medicine, University of Massachusetts Medical School, Worcester, Massachusetts, USA*

Xenopus laevis myosin 1d (*X*Myo1d) is a member of the myosin I class, subclass 4. Members of this class are single headed, bind calmodulin light chains and have lipid binding domains in their tails. The rat myo1d homologue has been implicated in endosome vesicle recycling in epithelial cells. Mutations in the *Drosophila* myosin 1d homologue cause *situs inversus* in the abdomen. The *X*Myo1d cDNA has been cloned and the derived amino acid sequence is 80% identical to the rat and human homologues. Sequence comparison revealed a novel isoform-specific tail homology embedded in the Tail Homology 1 (TH1) domain characteristic of myosin I isoforms. Western blot analysis using a polyclonal antibody raised against an isoform-specific peptide showed that the protein is present in eggs and levels increase at early neurula through tadpole stages. Whole mount *in situ* hybridization using a probe containing the 5′UTR (untranslated region) showed that *X*Myo1d mRNA is expressed in neural tube, pre-somitic mesoderm, somites and all three segments of cranial neural crest cells during their migration. Sections of the *in situ* hybridizations revealed that during somitogenesis, *X*Myo1d mRNA was localized to a stripe overlapping the nuclear region of somites during early tadpole stages.

Key words: left–right asymmetry; myosin 1d; myosin I; TH1; *Xenopus*.

Introduction

Members of the 18 different classes of myosin molecular motors have been found in all eukaryotes where they carry out various cell motility functions (Mooseker and Cheney 1995; Mermall *et al*. 1998; Sokac and Bement 2000; Berg *et al*. 2001; Foth *et al*. 2006). Several examples of the roles myosins can play have come from studying embryonic development in *Drosophila*. *Zipper*, a cellular myosin II, is required for dorsal closure (Franke *et al*. 2005), and is also a member of the apical cell polarity complex PAR3–PAR6–aPKC that mediates cell intercalation (Bertet *et al*. 2004) and localizes mRNAs encoding morphogens (Barros *et al*. 2003). Myosin VIIA nulls are also lethal, and weak loss-of-function alleles show hair and bristle defects (Kiehart *et al*. 2004). Myosin V mutants exhibit delayed development and die during third instar with no discernible morphological defects, although escapers show male infertility (Mermall *et al*. 2005).

Members of the myosin I family are single headed, bind calmodulin as their light chains and have a lipid-binding domain in their tails (Hammer 1994; Coluccio 1997). Myosin I isoforms exhibit a specific tail homology, TH1, which contains both actin and lipid binding domains (Hammer 1994; Lee *et al*. 1999). The lipid binding domains may be important in organizing local domains of membranes (Takeda and Chang 2005). Members of this family of myosins include the brush border isoform, myo1a (Mooseker and Coleman 1989); myo1c, the adaptation motor of the inner ear hair cell (Hasson *et al*. 1997; Batters *et al*. 2004); and myo1d (or *myr4*), originally found in rat neonatal brain, pyramidal cells and other tissues (Bähler *et al*. 1994) as well as in the axons of spinal neurons in rat neonates (Lund *et al*. 2005).

The *Drosophila* homologue of vertebrate myo1d, *Dm*Myo31DF, is the first actin-based motor shown to play a role in left–right asymmetry determination.

*Author to whom all correspondence should be addressed.
Email: Janine.LeBlancStraceski@merrimack.edu
Received 14 September 2008; revised 10 January 2009; accepted 20 February 2009.

Mutants exhibit complete *situs inversus* of gut and testes (Hozumi *et al*. 2006; Spéder *et al*. 2006). Myo1d is also involved in apical/baso-lateral vesicle transport in epithelial cells (Hubera *et al*. 2000). The results of work presented here have identified a myo1d isoform specific tail homology overlapping the TH1 lipid binding tail homology of the myosin I family as a potential target for investigation in these systems. In addition, the whole mount *in situ* hybridization expression pattern suggests that in frogs, the myosin 1d isoform may play multiple roles in the developing embryo.

Materials and methods

Cloning and sequence analysis

*Xl*Myo1d cDNA (GenBank Accession Number: AF540951) was obtained by several steps. First, an oocyte lambda library (Rebagliati *et al*. 1985) was screened by polymerase chain reaction (PCR). Forward and reverse primers for the screen (5′GAAGCCAGTAAGTACATC-ATGC3′; 5′TGTTTTTCACCCTCTCCACC3′) were derived from the isoform specific sequence in the head region that is flanked by the adenosine 5′-triphosphate (ATP)-binding site and conserved regions indicated in Figure 1(A) (Sokac and Bement 1998). Details of the screening protocol have been published (LeBlanc-Straceski *et al*. 2006). A single lambda clone, PS103, was obtained. The lambda insert was excised and subcloned into the *Eco*RI site of pGEM7f (Promega) to create pPS103. Sequencing and subsequent database comparisons revealed that the cDNA was truncated just after the head/tail junction, and was approximately 100 nucleotides short of the translational start site. The remaining 5′ and 3′ portions were obtained by rapid amplification of cDNA ends (RACE) (Invitrogen) and subcloned into pGEMT-Easy plasmid vectors (Promega). Sequencing of pJL5′-2 (5′ RACE clone) and pAOKB9 (3′ RACE clone) was carried out on intact plasmids and sets of nested deletions (Promega) by Iowa State University DNA Sequencing Facility.

Data analysis was carried out using basic local alignment search tool (BLAST) to search GenBank and the Conserved Domain Database (CDD) (Marchler-Bauer *et al*. 2005) of the National Center for Biotechnology Information (NCBI). Multiple sequence alignments and percent similarities were calculated using the ClustalW option of the MegAlign program of the Lasergene software package (DNASTAR).

PAGE and Western blot analysis

Protein samples were collected by lysing embryos in buffer (1% Triton X 100, 50 mM NaCl, 1 mM ethylenediaminetetraacetic acid (EDTA), 50 mM Tris, pH 7.6) plus protease inhibitors. One-half embryo equivalents were loaded per lane. Gels were transferred onto Immobilon (Millipore). A polyclonal antibody, Ab35, was raised in rabbits against a synthetic peptide (QED Bioscience). The sequence of the peptide corresponded to aa124-143 [NPSQRAEVERVKNMLLKSNC] located in the isoform-specific region of the head domain (see Fig. 1A). Blots were stripped according to the manufacturer's instructions and re-probed with anti-tubulin antibody (Cappell).

In situ *hybridization*

Whole mount *In situ* hybridization was carried out essentially as described (Harland 1991; Sive *et al*. 2000). Dig-UTP (Digoxygenin-Uridine triphosphate) labeled probes for *in situ* hybridization were synthesized (Promega, Life Technologies) from the 5′ end clone of *Xl*Myo1d obtained by RACE, pJL5′-2 (see section 2.1 above), which contains 591 bp of the 5′ UTR (untranslated region) plus 255 bp encoding the first 85 amino acids of the protein. BLASTN analysis of the protein encoding portion of the DNA sequence showed homology only to other myosin Id sequences in the GenBank database. *Xl*Myo1d sense probes were synthesized with T7 and antisense with SP6 RNA polymerase. The antisense actin probe was derived from pAC100 (Dworkin-Rastl *et al*. 1986) using SP6 RNA polymerase. Embryos previously subjected to whole mount *in situ* hybridization were embedded in paraplast and 10 μm sections cut and dehydrated, as described (Sive *et al*. 2000). Digital images were recorded using Kodak OpenLab Software and SPOT image capturing software.

Results

Domain structure of XlMyo1d

The *Xenopus* myosin 1d homologue has been cloned and sequenced. After an initial identification of the myo1d isoform by a TBLASTX GenBank sequence comparison, the *Xenopus* sequence was directly compared with five myosin I isoforms from humans. Table 1 shows that the *Xenopus* sequence was identified as a myo1d isoform due to its 90% homology to the human myo1d isoform as well as a much lower homology to all of the other myosin I isoforms. The derived amino acid sequence was then compared with four representative myo1d sequences: *Drosophila*, zebrafish, rat and human. Table 2, column 2, shows the percent amino acid sequence identity of *Xl*Myo1d to each of the other species. Comparison of the entire amino acid sequence shows that *Xl*Myo1d is most closely related to the

Fig. 1. Domain structure and amino acid sequence analysis of *Xenopus laevis* myosin 1d (XlMyo1d). (**A**) A comparison of the isoform-specific region between the invariant *GESGAGKT* and the very highly conserved *EAFGNAKT* sequences. Identical amino acids are highlighted. Sequences compared are myo1d isoforms from frog, *Xl*Myo1d (accession number: AF540952); fruit fly, *Dm*Myo31DF (accession number: S45573); zebrafish, *Dr*Myo1d (accession number: CAK11490); rat *Rn*Myo1d (originally identified as myr4) (accession number: X 71997); human, *Hs*MYO1D, (accession number: BC030602); and a myo1c isoform, *Hs*MYO1C (accession number: AAH44891). (**B**) The two IQ motifs previously reported for the myo1d subfamily were identified in *Xl*Myo1d. Sequences of several species were compared with the IQ motif consensus sequence from the myosin I family (I/V/L)QxxxRGxxx-(R/K)xx(F/I/L/V/W/Y) described previously (Bähler and Rhoads 2002). Positions of conserved amino acids are designated by asterisks in the alignment, and amino acids found in the consensus sequence are shaded. (**C**) The TH1 of the myosin I family was compared with representative members of the myo1d subfamily using the ClustalW sequence comparison program. The top row shows the TH1 consensus sequence obtained from the CDD (Conserved Domain Database) of National Center for Biotechnology Information (NCBI). The second row shows a myo1d tail consensus sequence, which was obtained by comparing representative sequences from fly, fish, frog, and rat. Shaded amino acids are identical to the TH1 (top row). Bold amino acids are identical to the myo1d tail consensus.

A. Isoform Specific Region in the Head Domain

```
XlMyo1d      GESGAGKT EASKYIMQYIAAITNPSQRAEVERKNMLLKSNCVL EAFGNAKT 153
DmMyo31DF    GESGAGKT EASKIIMKYIAAVTNAQGQNEIERKNVLIQSNAIL ETFGNAKT 151
DrMyo1d      GESGAGKT EASKYIMQYIAAITNPSQRAEVESKNVLLKSNCVL EAFGNAKT 153
RnMyo1d      GESGAGKT EASKYIMQYIAAITNPSQRAEIERKNMLLKSNCVL EAFGNAKT 153
HsMYO1D      GESGAGKT EASKYIMQYIAAITNPSQRAEVERKNMLLKSNCVL EAFGNAKT 153
HsMYO1C      GESGAGKT EATKRLLQFYAETCPAPERGGAVRDR LLQSNPVL EAFGNAKT 154
```

B. IQ Motifs

```
                 **   **   *  *
XlMyo1d      IILFLQKLWRGTLARRRC     718
DmMyo31DF    IVTLLQKRVRGWIVRRNF     713
DrMyo1d      LVLFLQKVWRGALARMRC     720
RnMyo1d      VVLFLQKVWRGTLARMRY     718
HsMYO1D      IVLFLQKVWRGTLARMRY     718

                **   **   *  *
XlMyo1d      AGLTILRYYRRYKVKSYL     740
DmMyo31DF    AAITIVRAYKAYKLRSYV     735
DrMyo1d      AIYTIMGYYKCYKVKAHF     742
RnMyo1d      AALTIIRYYRRYKVKSYI     740
HsMYO1D      AALTIIRYYRRYKVKSYI     740
```

C. Tail Homologies

```
Myosin 1 TH1     -QKVQASEILKGKKERRRQSVNRKFVGDYLG-LEENP---     35
Myo1d tail       RAKVAAFEALKGX--RXDWGLQRXWEGDYLASXQDNPXXX     38

XlMyo1d          RAKVAAFENLKGH--RVDMGLQGCWEGSYLASNQENARN-    837
DdMyo31DF        RLQIIAATALAGR--RPYWGQARRWVGDYLANSQENSGYE    833
DrMyo1d          RAKVAAFSALSGE--RMDWGYSRSWERDYLANAKDSPLM-    839
RnMyo1d          RAKVAAMEMLKGQ--RADLGLQRAWEGNYLASKPDTPQT-    837
HsMYO1D          RAKVAAVEMLKGQ--RADLGLQRAWEGNYLASKPDTPQT-    837

Myosin 1 TH1     -------KLQKALGSEEGKEKVLFADKVNKFNRSGKPSKR     68
Myo1d tail       XXSGXFVXIXNELKRKDKFMQVLFSSHVRKVNRFNKVXDR     78

XlMyo1d          --SNQFVSRSNELQRKDKFMQALFSCHVQKVNRFNKVQDR    875
DdMyo31DF        AYNGSIKNIRNHPADGETFQQVLFSSFVKKFNHFNKQANR    873
DrMyo1d          --SSNFVRITKELKNKDQYGQVLFSSAVRMLNWFNNTKDR    877
RnMyo1d          --SGTFVPVANELKRKDKYMNVLFSCHVRKVNRFSKVEDR    875
HsMYO1D          --SGTFVPVANELKRKDKYMNVLFSCHVRKVNRFSKVEDR    875

Myosin 1 TH1     ILLLTDRALYLVGREDQKTYVLKRRIPLSAITSVSLSSLS    108
Myo1d tail       AIFVTDRHLYKLDXXPXKXYKVMKTIPLYNVTGLSVSSGK    118

XlMyo1d          AIFITDRHLYKMD--FGKEYKVMTSTPLYNVSGISVTSGK    913
DdMyo31DF        AFIVSDSTIHKLDGIKNKFKDMKRTIKIRELTSISVSPGR    913
DrMyo1d          ALLITDKHIYRLE--FKKHFKVQKRIALDSVVGLSVTSGS    915
RnMyo1d          AIFVTDRHLYKMD--FTKQYKVMKTIPLYNLTGLSVSNGK    913
HsMYO1D          AIFVTDRHLYKMD--FTKQYKVMKTIPLYNLTGLSVSNGK    913

Myosin 1 TH1     DDLFVIHVSGEGDLVLES---------DFKTELVTVLVKH    139
Myo1d tail       DQLVVFHTKDNKDLIVCLXXGXQPFXESRIGELVGVLXNH    158

XlMyo1d          DQLVVFHMKDNKDLIVCLGCGQGFYDSRIGELVGVLANH    953
DdMyo31DF        DQLIVFHSSKNKDLVFSLESEYTFLKEDRIGEVVGIVCKK    953
DrMyo1d          DQLVVLHTATQDDFLVHLQRGQLNFNQDRVGELS------    949
RnMyo1d          DQLVVFHTKDNKDLIVCL-FGKQPTHESRIGELVGVLVNH    952
HsMYO1D          DQLVVFHTKDNKDLIVCL-FGKQPTHESRIGELVGVLVNH    952

Myosin 1 TH1     YKSATGGKLPVNFSDS-IEYRLKKGKTRTVTFQKDEGSGA    178
Myo1d tail       FKXSTXRPLQVNVTXF-IQCRLH-GKXCSITVETK--XNQ    194

XlMyo1d          FK-SERRPLQVTVSHF-IQCRQH-GRSCSITVETK--INQ    988
DdMyo31DF        YHDLTGTELRVNVTTN-ISCRLD-GKARIITVEAA--SNV    989
DrMyo1d          ------TPLPVKVCSTGLQVQMG-GKPKSITVETK--PGQ    980
RnMyo1d          FK-SEKRHLQVNVTNF-VQCSLH-GKKCTVSVETR--LNQ    987
HsMYO1D          FK-SEKRHLQVNVTNF-VQCSLH-GKKCTVSVETR--LNQ    987

Myosin 1 TH1     ELPIFKSKKGHVVSIAPG                          196
Myo1d tail       XQPDFTKNRXGFILSVFAN                         216

XlMyo1d          SQPQFTKNRAGFTLSVPAN                        1007
DdMyo31DF        EVPNFRPKEGNIIFEVPAAYCV                     1011
DrMyo1d          TISDFKKSRTGFTLLLPQ                          998
RnMyo1d          PQPDFTKNRSGFILSVPGN                        1006
HsMYO1D          PQPDFTKNRSGFILSVPGN                        1006
```

Table 1. Assignment of *Xenopus laevis* myosin 1d (XlMyo1d) isoform identity

*Xl*Myo1d Vs:	Identity (%)	Homology (%)
Human myo1a	39	56
Human myo1b	45	64
Human myo1c	42	59
Human myo1d	80	90
Human myo1e	42	61

Derived amino acid sequences from five myosin I isoforms from humans were compared with *Xl*Myo1d using the Blastp (BLOSUM62) program. GenBank accession numbers for the human sequences are *Hs*MYO1A (NP_005370); *Hs*MYO1B (NP_001123630); *Hs*MYO1C (AAH44891); *Hs*MYO1D (NP_056009 XP_050041); *Hs*MYO1E (NP_004989).

Table 2. Percent amino acid sequence identity of full length and conserved domains of Myo1d homologues

	Identity (%)			
	Overall	Head consensus	TH1	Myo1d tail consensus
*Xl*Myo1d	–	100	30	74
*Dm*31DF	51.8	61	33	42
*Dr*Myo1d	64.5	94	28	52
*Rn*Myo1d	80.1	97	33	78
*Hs*MYO1D	80.3	100	33	78

Derived amino acid sequences from frog (*Xl*Myo1d), fruit fly (*Dm*31DF), rat (*Rn*Myo1d) and human (*Hs*MYO1D) were compared using the ClustalW (Thompson *et al*. 1994). The myosin 1d head conserved region consensus was derived by comparing all five sequences shown in Figure 1(A), excluding the motifs in italics. TH1 (pfam06017, Myosin_2_tail) sequence was obtained from the Conserved Domain Database of National Center for Biotechnology Information (NCBI) (Marchler-Bauer *et al*. 2005). The myo1d tail consensus was derived by comparing amino acid sequences of four tail regions: frog, fly, fish and rat. Human was excluded because it was identical to rat and would have biased the consensus.

mammalian homologues, followed by fish and then fly. This same order is preserved when comparing the isoform specific region in the head (Bement *et al*. 1994) (Table 2, column 3), and a myo1d tail consensus sequence (Table 2, column 5). However, all five isoforms had approximately 30% identity to the TH1 (Table 2, column 4).

Myosins are defined as actin-activated ATPases. The head domain of myosin contains the enzymatic properties of the molecule. Because these functions define the entire superfamily of molecules, the amino acids that comprise the head domain are very highly conserved among all myosins. However, isoform specific regions have been identified within the head domain. Figure 1(A) shows the sequence alignment of an isoform specific region of the head that lies between the two highly conserved regions. The ATP binding domain, GESGAKT, is invariant in all myosins, and forms the amino terminal boundary of the isoform specific region in the head domain (Bement *et al*. 1994). The carboxyl terminal end is bound by the sequence EAFGNAKT, which is also very highly conserved. Note that only *Dm*31DF has a single, conservative amino acid substitution in this motif. The amino acid sequence found between these two motifs is isoform specific. Table 2 shows that the highest degree of identity occurs in this small region of 35 amino acids. Figure 1(A) shows that this region of *Xl*Myo1d is identical to human, and varies by only one and two amino acids from rat and zebrafish, respectively. By comparison, Figure 1(A) shows that this same region diverges dramatically from the closely related myo1c isoform.

XlMyo1d has two IQ motifs

Many myosin heavy chains bind calmodulin as their light chain via the IQ motif. This motif can be repeated several times, depending on the myosin class. Multiple repeats have been associated with increasing numbers of calmodulin. For example, a myosin V from yeast contains two heavy chains, each with six IQ motifs organized in pairs, and a total of 12 calmodulin or calmodulin-like light chains (Terrak *et al*. 2005). Figure 1(B) shows the two motifs found in *Xl*Myo1d specifically and in the myo1d family in general. In the *Xl*Myo1d heavy chain, the motifs are separated by only four amino acids. IQ1 is more homologous to the consensus sequence (Rhoads and Friedberg 1997; Bähler and Rhoads 2002). However, in rat myo1d, both IQ motifs function in binding calmodulin (Bähler *et al*. 1994; Köhler *et al*. 2005). It is likely that these two *Xenopus* IQ motifs also bind calmodulin light chains.

TH1 and a myo1d tail homology in XlMyo1d

Figure 1(C) shows the location of TH1 in the *Xl*Myo1d tail. Table 1, column 4, shows that the sequences analyzed have similar levels of homology, approximately 30%, to the TH1 consensus. The alignment of the other 1d myosins shows that there are several other highly conserved residues within this subclass, that are not present in the TH1 consensus. Based on the comparison of four representatives, *Xl*Myo1d, *Dm*34DF, *Dr*Myo1d and *Rn*Myo1d, a consensus tail sequence for the myo1d family was derived. (*Hs*MYO1D is identical to *Rn*Myo1d in this region and was not included to avoid biasing the consensus). Table 1, column 5, shows that *Xl*Myo1d and the other myo1d representatives

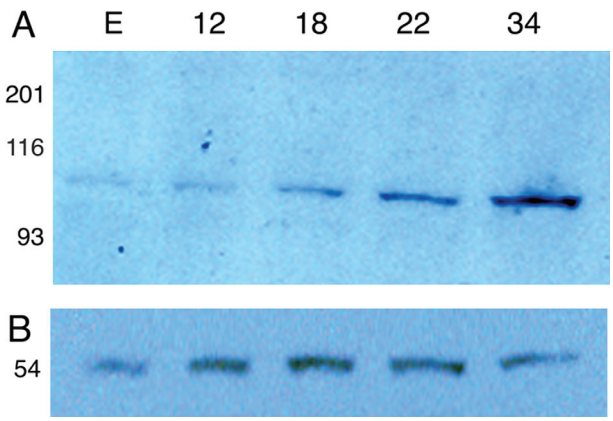

Fig. 2. *Xenopus laevis* myosin 1d (*Xl*Myo1d) expression increases during early development. Protein samples were prepared from various stages of embryogenesis and analyzed by Western blot. One half-embryo equivalents were loaded into lanes of a 7.5% polyacrylamide gel. (**A**) The rabbit polyclonal antibody, Ab35, identified a protein product of the predicted molecular weight, for *Xl*Myo1d, 116 kDa. (**B**) An anti-tubulin antibody was incubated with the stripped blot to control for gel loading.

are more closely related to the 1d consensus than to the TH1 consensus, which was derived from the entire myosin I family.

XlMyo1d protein expression increases through development

A synthetic peptide from the conserved head region (Fig. 1A) served as antigen for a polyclonal antibody used in Western blot analysis shown in Figure 2(A). A 116-kDa protein corresponding to the molecular weight predicted from the sequence was detected. This protein was present in eggs and increased in amount through stage 34 indicating both maternal and embryonic expression. The increase in expression beginning at stage 18 and continuing through development correlates with the *in situ* data presented in Figure 3. Anti-tubulin antibody was used to show equal loading (Fig. 2B).

XlMyo1d is expressed in neural tube, somites and cranial neural crest cells of early tadpole

Whole mount *in situ* hybridization was carried out on various stages of *Xenopus* embryos using an antisense probe containing the 5′ UTR and a portion of the amino acid encoding sequence. Figure 3(A–K) shows both neural and mesodermal expression of *Xl*Myo1d. Figure 3(A) shows that at the yolk plug stage (Nieukoop and Faber 1994, stage 12) no localized staining was visible. Localized expression was not detected until stage 17, when somites begin to form (Hausen and Reibesell 1991). By stage 20 the embryo has between six and seven somites and expression could be detected in somites, neural tube and in cranial neural crest cells (Fig. 3B,C).

Neural tube expression was also detected in late neurula (Fig. 3B) through tadpole stages (Fig. 3H–K). Staining is faint and diffuse early (Fig. 3B,F), but intensifies in anterior portions (Fig. 3H,K). This pattern is consistent with *Xl*Myo1d expression in rat neonatal brain (Bähler *et al*. 1994) and spinal neurons (Lund *et al*. 2005).

At stage 20, cranial neural crest cells are still located near the anterior dorsal mid-line, and have not segregated into distinct clusters (Sadaghiani and Thiebaud 1987). Between stages 20.5 and 22 (Fig. 3D,E) staining of the three compartments of the cranial neural crest cells was evident as they migrated toward the branchial arch and mandibular regions. All three segments of cranial neural crest cells (anterior to posterior: mandibular, hyoid and branchial) showed *Xl*Myo1d expression. As development progresses, the mandibular segment splits and part of it surrounds the optic vesicle, while the other portion forms the mandibular arc between the cement gland and the optic vesicle (Sadaghiani and Thiebaud 1987). As seen in Figure 3(I,J,E), *Xl*Myo1d expression is detected in both of these cell populations. By stage 30, *Xl*Myo1d is also detected in cells surrounding the otic vesicle (Fig. 3I–J). Control hybridizations with *Xl*Myo1d sense probe showed no detectible staining (Fig. 3L). Actin expression was detected in tissue destined to become muscle (somites) and heart (Fig. 3M).

XlMyo1d mRNA is concentrated in the nuclear region of pre-somitic mesoderm and somites

Somitic and pre-somitc expression of *Xl*Myo1d was evident in stages 17 to late tadpole. Figure 3(B–I) shows a distinct stripe of staining in each somite. By stage 22 (Fig. 3F,G) *Xl*Myo1d levels in both pre-somitic and somitic tissue increased relative to earlier stages. This figure shows clearly *Xl*Myo1d expression in a stripe near the dorsal midline in pre-somitic tissue and a stripe in each somite. By stage 30 (Fig. 3H,I), somitic expression is still evident.

From the whole mount embryos it was difficult to determine where in the somite the *Xl*Myo1d mRNA expression was concentrated. Therefore, whole mount *in situ* hybridization was carried out and embryos were paraffin embedded and sectioned. Figure 4 shows phase micrographs of 10 μm, horizontal sections. Figure 4(A) shows actin mRNA distributed evenly throughout the cytoplasm. Figure 4(B,C) shows sections from an embryo hybridized to the myosin probe. Somites are approximately 70 μm wide along the A-P axis and

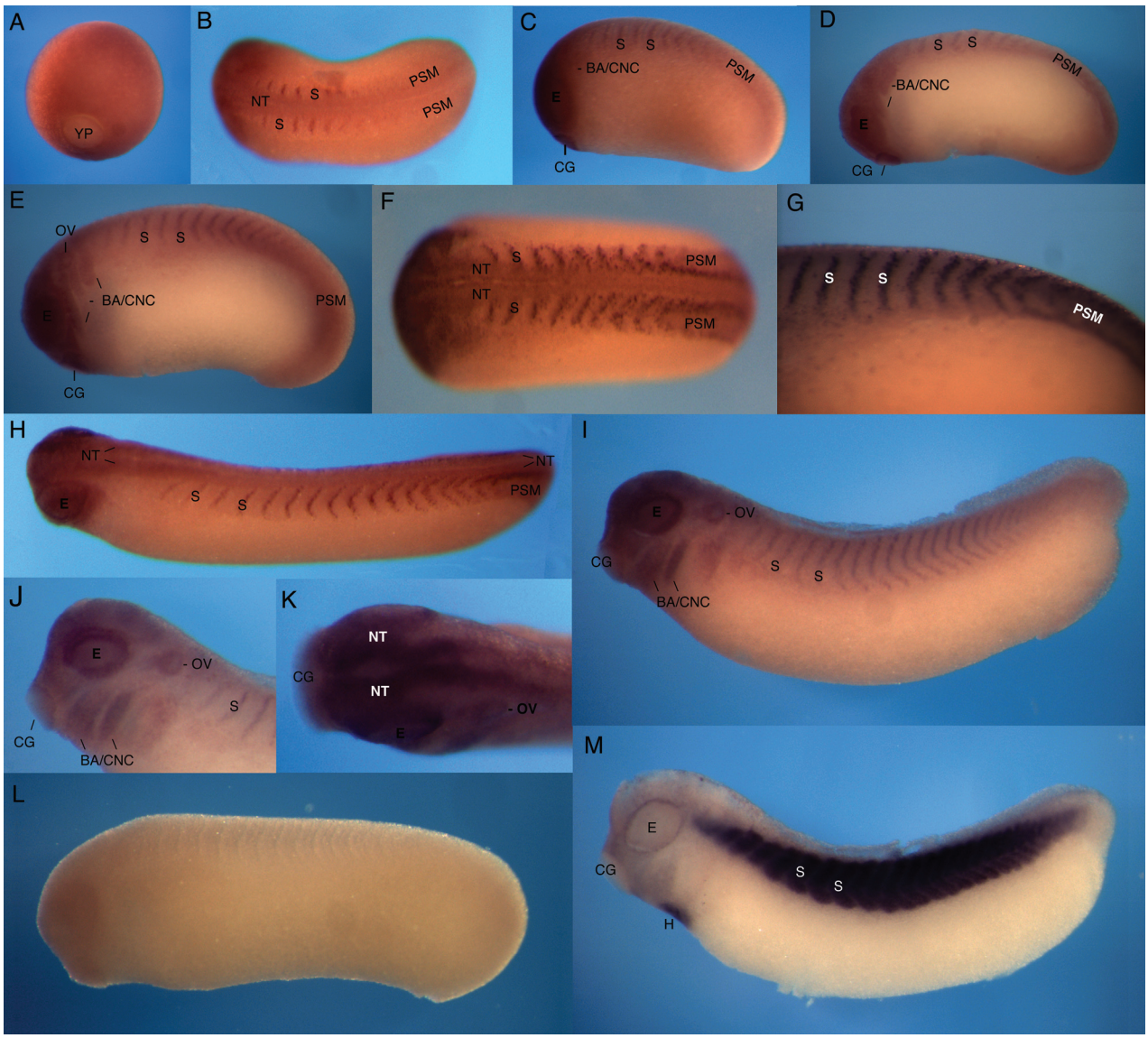

Fig. 3. *Xenopus laevis* myosin 1d (*X*Myo1d) expression is detected in somites, neural tissue and neural crest. *X*Myo1d mRNA expression was detected using whole mount *in situ* hybridization. (**A–K**) Embryos hybridized to the *X*Myo1d probe. (**A**) Stage 12. Yolk plug stage. (**B**) Stage 20, dorsal view. (**C**) Stage 20, lateral view, showing mandibular, hyoid and branchial neural crest cells, anterior to posterior. (**D**) Stage 20.5 lateral view. (**E–G**) Stage 22. (**E**) Side view. (**F**) Dorsal view. (**G**) Lateral view, at higher magnification. The rotation of the cells during the formation of the somite in an anterior to posterior direction is detected. (**H–K**) Stage 30. (**H**) Dorsal, oblique view. (**I**) Lateral view. (**J**) Lateral view close-up of the head region. (**K**) Close up of the head, dorsal view. (**L**) Stage 26 embryo hybridized to *X*Myo1d sense probe. (**M**) Stage 30 embryo hybridized to the actin probe. BA/CNC, branchial arch region and cranial neural crest segments; CG, cement gland; E, eye; H, heart; NT, neural tube; OV, otic vesicle; PSM, pre-somitic mesoderm; S, somite; YP, yolk plug.

90 μm long in the proximal to distal dimension. Somites are organized as stacks of cylindrical cells with the long dimension parallel to the anterior posterior (A–P) axis (Hausen and Reibesell 1991). Nuclei line up in the centers of the stacks of cells. In pre-somitic tissue the cells are rotated 90° so that their long axis is perpendicular to the A-P axis. The rotation of this tissue can be detected by the pattern of *X*Myo1d mRNA expression (Figs 3F, 4B). Figure 4(C) is a higher magnification showing the concentration of staining over the nuclei.

Discussion

Myosin family members have been shown to play specific key roles in embryonic development. In order to determine what roles myo1d might play in a vertebrate

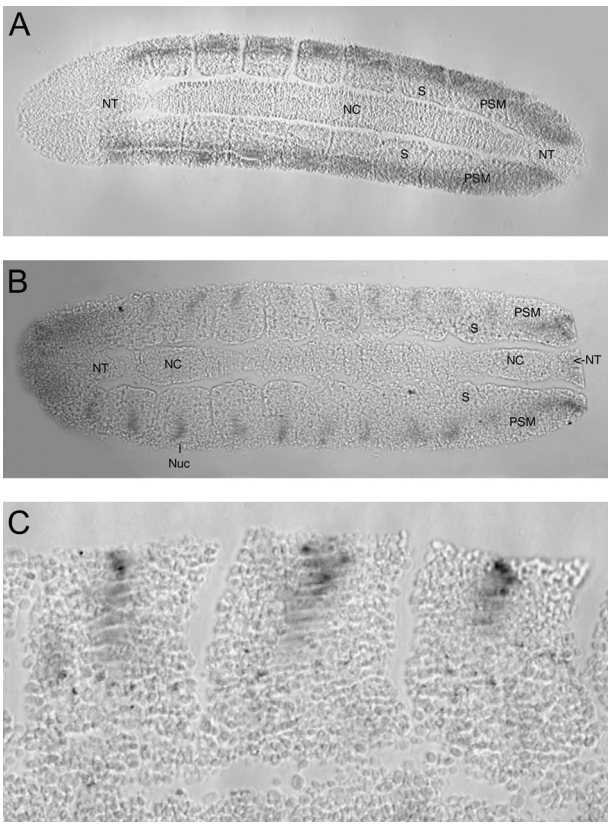

Fig. 4. *Xenopus laevis* myosin 1d (*Xl*Myo1d) expression is detected in the nuclear region of somites and pre-somitic mesoderm. Horizontal, 10 μm sections were taken from embryos that had undergone whole mount *in situ* hybridization to the *Xl*Myo1d and actin probes. Head is left and tail is right. Since the dorsal side of the embryo is curved, only the anterior-most and posterior-most portions of the neural tube and notochord are present in the sections shown in (**A**) and (**B**). (**A**) Actin probe hybridization. (**B–C**) *Xl*Myo1d probe. (**C**) Somite structure at a higher magnification than shown in (**B**). Each somite measures 70 μm anterior to posterior and 90 μm proximal to distal. NC, notochord; NT, neural tube; Nuc, nuclei of somite; PSM, pre-somitic mesoderm; S, somite.

system, the *Xenopus* cDNA sequence was analyzed and the tissue specific pattern of expression was determined during early development. Myosin heads, except for the isoform specific region (Bement *et al*. 1994) possess a homology that reflects the domain's universal actin-activated ATPase function. Tails, however, are diverse. Within this diversity, several different domains have been identified, sometimes appearing across different classes of myosin (Foth *et al*. 2006; Odronitz and Kollmar 2007). All members of the myosin I class have a TH1 domain that binds lipids (Hammer *et al.* 1994; Coluccio 1997). Comparison of the *Xl*Myo1d cDNA sequence to other vertebrate orthologues revealed a strong overall homology as well as other common domains such as conserved myosin sequences in the head region, and IQ motifs in the neck region. A myo1d isoform specific sequence in the head domain was also identified. In addition, a myo1d isoform specific consensus sequence embedded within the lipid binding TH1 domain was newly identified. One possible role for this domain is in the transport of specific vesicles during trafficking in epithelia (Hubera *et al*. 2000) or other polarized cells, or in the creation of specific lipid domains within membranes (Takeda and Chang 2005). Further structure/function investigation will determine whether this domain provides the myo1d family of proteins with specific lipid binding capabilities, unique to this isoform.

The high degree of conservation between orthologues as distant as *Drosophila* and humans suggests that this myosin has similar roles in all organisms. Since *Drosophila* mutations cause *situs inversus*, one such role may be in vesicle transport during the process of asymmetry formation, such as proposed by Tanaka *et al*. (2005). The establishment of left–right asymmetry is achieved by creating a gradient of Sonic hedgehog (Shh) and retinoic acid at the node. Cilia at the node propel NVPs (nodal vesicular parcels), extracellular vesicles carrying the signaling molecules, from right to left across the node. Once they reach the left side, NVPs are broken open and signal transduction is mediated by microvilli. (Tanaka *et al*. 2005). The role myo1d might play in NVP intracellular trafficking in the signal producing cells on the right side of the node warrants further investigation.

Our *in situ* data show that developing frog neural tissue has a high concentration of *Xl*myo1d. A similar localization has been detected in rat neonates (Bähler *et al*. 1994). Since myo1d has been shown to play a role in endocytic traffic in MDCK cells (Hubera *et al*. 2000), it may play a similar role in vesicle transport in neural tissue as well. Neurons, like epithelial tissue, have distinct cellular polarity. An intriguing possibility to investigate is whether the myo1d tail homology may be involved in signaling endosome traffic in neural tissue. Although antero- and retrograde axonal transport is microtubule based, vesicular traffic at the cell cortex of the synapse and in the dendrites is actin based. Signaling endosomes collect neurotrophins at the synapse and transport them to the cell body using a mechanism that is at least partially actin based (Weible and Hendry 2004; Yano and Chao 2004; Bronfman *et al*. 2007). It remains to be determined exactly how, if at all, myo1d is involved in this particular process.

Regulation by Ca^{++}/calmodulin binding may be critical for *Xl*myo1d function. Two IQ motifs were identified in *Xl*Myo1d, similar to those detected in the orthologues from other species. IQ motifs bind calmodulin or calmodulin-like light chains, usually in a 1 : 1 ratio. Anywhere from one to eight copies can be present,

but typically two to six are found in many classes of myosin (see Odronitz and Kollmar 2007). Since myo1d is involved in cytoplasmic vesicle transport in epithelial cells, and membrane traffic in MDCK cells is regulated, in part, by myo1d and calmodulin binding (Hubera *et al*. 2000), *Xl*myo1d may also transport vesicles in neural tissue in a Ca^{++}/calmodulin dependent manner. In addition, data are beginning to emerge that calcium regulation of myosin ATPase activity and motility may be mediated through the binding and release of the calmodulin light chains (Manceva *et al*. 2007). Further investigation will reveal whether Ca^{++}/calmodulin regulation is important in *Xl*Myo1d function during embryonic development.

The pattern of *Xl*Myo1d expression suggests multiple roles for this myosin in amphibian development. The mRNA of *Xl*Myo1d was found in several different tissues of both ecto- and mesodermal origin. Expression in the neural tube and brain is consistent with previous localization studies in rats (Bähler *et al*. 1994). However, *Rn*Myo1d was detected only in neonates, not in embryos. It is interesting that in frogs, *Xl*Myo1d expression was detected in cranial neural crest cells but not trunk neural crest. This suggests a role that is specific for this subset of neural crest. Somites, cells of mesodermal origin, also show expression of *Xl*Myo1d. The detection of *Xl*Myo1d mRNA in two populations of cells that undergo dramatic tissue rearrangements based on the movement of individual cells – cranial neural crest cells and somitic cells – suggest that one role of *Xl*Myo1d may be in cell migration.

Note in added proof

Subsequent to the submission of the sequence for *Xl*Myo1d, another *Xenopus* myo1d sequence was deposited in GenBank (Klein *et al*. 2002; Accession Number: BC073240). These two sequences differ by only five amino acid substitutions, which probably represent natural polymorphisms in the captive laboratory population.

Acknowledgments

This manuscript is dedicated to the memory of Sharon Ricketts Betz, a wonderful student, scientist and human being. She is sadly missed by colleagues, friends and family. Sharon Rickets, Martha-Rachel Knittel, Angela Kulesza, Amy O'Connell, and authors Pablo Sobrado and Laura Lemoine, all contributed key data to this manuscript while undergraduates at Merrimack College. Thanks to Sergei Sokol and to all the members of his lab for patient technical assistance and thoughtful discussions; and to Lynne Coluccio for a critical reading of the manuscript. Several undergraduate laboratory sections from BI338 Cellular Biochemistry II: Nucleic Acids also carried out intermediate cloning steps. This work is supported by grants from the National Science Foundation, NSF-RUI 0077516 (JML-S) and an REU (AC); a Merck/AAAS Summer Undergraduate Research Program (SURP) award (AK, JML-S); Sigma Xi GIARs (AC, AK and LL); a Murray Fellowship Award (JML-S); and the Faculty Development Grant Program of Merrimack College (JML-S).

References

Bähler, M. & Rhoads, A. 2002. Calmodulin signaling via the IQ motif. *FEBS Lett*. **513**, 107–113.

Bähler, M., Kroschewski, R., Stoffler, H. E. & Behrmann, T. 1994. Rat myr 4 defines a novel subclass of myosin I: identification, distribution, localization, and mapping of calmodulin-binding sites with differential calcium sensitivity. *J. Cell Biol*. **126**, 375–389.

Barros, C. S., Phelps, C. B. & Brand, A. H. 2003. *Drosophila* nonmuscle myosin II promotes the asymmetric segregation of cell fate determinants by cortical exclusion rather than active transport. *Dev. Cell* **5**, 829–840.

Batters, C., Wallace, M. I., Coluccio, L. M. & Molloy, J. E. 2004. A model of stereocilia adaptation based on single molecule mechanical studies of myosin I. *Philos. Trans. R. Soc. Lond. B. Biol. Sci*. **1452**, 1895–1905.

Bement, W. M., Hasson, T., Wirth, J. A., Cheney, R. E. & Mooseker, M. S. 1994. Identification and overlapping expression of multiple unconventional myosin genes in vertebrate cell types. *Proc. Natl Acad. Sci. USA* **91**, 6549–6553.

Berg, J. S., Powell, B. C. & Cheney, R. E. 2001. A millennial myosin census. *Mol. Biol. Cell* **12**, 780–794.

Bertet, C., Sulak, L. & Lecuit, T. 2004. Myosin-dependent junction remodeling controls planar cell intercalation and axis elongation. *Nature* **429**, 667–671.

Bronfman, F. C., Escudero, C. A., Weis, J. & Kruttgen, A. 2007. Endosomal transport of neurotrophins: roles in signaling and neurodegenerative diseases. *Dev. Neurobiol*. **67**, 1183–1203.

Coluccio, L. M. 1997. Myosin I. *Amer. J. physiol*. **273**, C347–C359.

Dworkin-Rastl, E., Kelley, D. B. & Dworkin, M. B. 1986. Localization of specific mRNA sequences in *Xenopus laevis* embryos by *in situ* hybridization. *J. Embryol. Exp. Morph*. **91**, 153–168.

Foth, B. J., Goedecke, M. C. & Soldati, D. 2006. New insights into myosin evolution and classification. *Proc. Natl Acad. Sci., USA* **103**, 3681–3686.

Franke, J. D., Montague, R. A. & Kiehart, D. P. 2005. Nonmuscle myosin II generates forces that transmit tension and drive contraction in multiple tissues during dorsal closure. *Curr. Biol*. **15**, 2208–2221.

Hammer, J. A. III. 1994. The structure and function of unconventional myosins: A review. *J. Muscle Res. Cell Motility* **15**, 1–10.

Harland, R. M. 1991. *In situ* hybridization: an improved whole-mount method for *Xenopus* embryos. *Methods. Cell Biol*. **36**, 685–695.

Hasson, T., Gillespie, P. G., Garcia, J. A., MacDonald, R. B., Zhao, Y., Yee, A. G., Mooseker, M. S. & Corey, D. P. 1997. Unconventional myosins in inner-ear sensory epithelia. *J. Cell Biol*. **137**, 1287–1307.

Hausen, P. & Reibesell, M. 1991. *The Early Development of Xenopus Laevis*. Springer Verlag, New York.

Hozumi, S., Maeda, R., Taniguchi, K., Kanai, M., Shirakabe, S., Sasamura, T., Spéder, P., Noselli, S., Aigaki, T., Murakami, R. & Matsuno, K. 2006. An unconventional myosin reverses the default handedness in visceral organs. *Nature*. **440**, 798–802.

Hubera, L. A., Fialkaa, I., Paihaa, K., Hunzikerb, W., Sacksc, D. B., Bähler, M., Waye, M., Gagescuf, R. & Gruenbergf, J. 2000. Both calmodulin and the unconventional myosin Myr4 regulate membrane trafficking along the recycling pathway of MDCK cells. *Traffic* **1**, 494–503.

Kiehart, D. P., Franke, J. D., Chee, M. K., Montague, R. A., Chen, T., Roote, J. & Ashburner, M. 2004. *Drosophila crinkled*, mutations of which disrupt morphogenesis and cause lethality, encodes fly myosin VIIA. *Genetics* **168**, 1337–1352.

Klein, S. L., Strausberg, R. L., Wagner, L., Pontius, J., Clifton, S. W. & Richardson, P. 2002. Genetic and genomic tools for *Xenopus* research: The NIH *Xenopus* initiative. *Dev. Dyn*. **225**, 384–391.

Köhler, D., Struchholz, S. & Bähler, M. 2005. The two IQ-motifs and Ca2+/calmodulin regulate the rat myosin 1d ATPase activity. *FEBS J*. **272**, 2189–2197.

LeBlanc-Straceski, J., Sobrado, P., Betz, S., Donoghue, J. & Morgan, K. 2006. The lift pool method for isolation of cDNA clones from lambda phage libraries. *Electronic J. Of Biotech*. [online]. 9. Available from: http://www.ejbiotechnology.info/content/vol9/issue4/full/2/.

Lee, W.-L., Ostap, E. M., Zot, H. G. & Pollard, T. D. 1999. Organization and ligand binding properties of the tail of *Acanthamoeba* myosin-Ia identification of an actin-binding site in the basic (tail homology-1) domain. *J. Biol. Chem*. **274**, 35159–35171.

Lund, L. M., Machado, V. M. & McQuarrie, I. G. 2005. Axonal isoforms of myosin-I. *Biochem. Biophys. Res. Commun*. **330**, 857–864.

Manceva, S., Lin, T., Pham, H., Lewis, J. H., Goldman, Y. E. & Ostap, E. M. 2007. Calcium regulation of calmodulin binding to and dissociation from the myo1c regulatory domain. *Biochemistry* **46**, 11718–11726.

Marchler-Bauer, A., Anderson, J. B., Cherukuri, P. F., DeWeese-Scott, C., Geer, L. Y., Gwadz, M., He, S., Hurwitz, D. I., Jackson, J. D., Ke, Z., Lanczycki, C. J., Liebert, C. A., Liu, C., Lu, F., Marchler, G. H., Mullokandov, M., Shoemaker, B. A., Simonyan, V., Song, J. S., Thiessen, P. A., Yamashita, R. A., Yin, J. J., Zhang, D. & Bryant, S. H. 2005. CDD: A Conserved Domain Database for protein classification. *Nucleic Acids Res*. **33**, D192–D196.

Mermall, V., Post, P. L. & Mooseker, M. S. 1998. Unconventional myosins in cell movement, membrane traffic, and signal transduction. *Science*. **279**, 527–533.

Mermall, V., Bonafé, N., Jones, L., Sellers, J. R., Cooley, L. & Mooseker, M. S. 2005. *Drosophila* myosin V is required for larval development and spermatid individualization. *Dev. Biol*. **286**, 238–255.

Mooseker, M. S. & Cheney, R. E. 1995. Unconventional myosins. *Annu. Rev. Cell Dev. Bio*. **11**, 633–675.

Mooseker, M. S. & Coleman, T. R. 1989. The 110-kD protein-calmodulin complex of the intestinal microvillus (brush border myosin I) is a mechanoenzyme. *J. Cell Biol*. **108**, 2395–2400.

Nieukoop, P. D. & Faber, J. 1994. *Normal Table of Xenopus Laevis (Daudin)*. Garland Publishing, New York.

Odronitz, F. & Kollmar, M. 2007. Drawing the tree of eukaryotic life based on the analysis of 2269 manually annotated myosins from 328 species. *Genome. Biol*. **8**, R196. http://genomebiology.com/2007/8/9/R196.

Rebagliati, M. R., Weeks, D. L., Harvey, R. P. & Melton, D. A. 1985. Identification and cloning of localized maternal RNAs from *Xenopus* eggs. *Cell* **42**, 769–777.

Rhoads, A. R. & Friedberg, F. 1997. Sequence motifs for calmodulin recognition. *FASEB J*. **11**, 331–340.

Sadaghiani, B. & Thiebaud, C. H. 1987. Neural crest development in the *Xenopus laevis* embryo, studied by interspecific transplantation and scanning electron microscopy. *Dev. Biol*. **124**, 91–110.

Sive, H. L., Grainger, R. M. & Harland, R. M. 2000. *Early Development of Xenopus Laevis*. Cold Spring Harbor Laboratory Press, New York.

Sokac, A. M. & Bement, W. M. 1998. Identification of multiple signaling myosins in the *Xenopus* oocyte. *Mol. Biol. Cell* (Suppl.)(9), 388a.

Sokac, A. M. & Bement, W. M. 2000. Regulation and expression of metazoan unconventional myosins. *Int. Rev. Cytol*. **200**, 197–304.

Spéder, P., Ádám, G. & Noselli, S. 2006. Type ID unconventional myosin controls left–right asymmetry in *Drosophila*. *Nature* **440**, 803–807.

Takeda, T. & Chang, F. 2005. Role of fission yeast myosin I in organization of sterol-rich membrane domains. *Current Biol*. **15**, 1331–1336.

Tanaka, Y., Okada, Y. & Hirokawa, N. 2005. FGF-induced vesicular release of Sonic hedgehog and retinoic acid in leftward nodal flow is critical for left–right determination. *Nature*. **435**, 172–177.

Terrak, M., Rebowski, G., Lu, R., Grabarek, Z. & Dominguez, R. 2005. Structure of the light chain-binding domain of myosin V. *Proc. Natl Acad. Sci. USA* **102**, 12718–12723.

Thompson, J. D., Higgins, D. G. & Gibson, T. J. 1994. CLUSTAL W: Improving the sensitivity of progressive multiple sequence alignment through sequence weighting, position-specific gap penalties and weight matrix choice. *Nucleic Acids Res*. **22**, 4673–4680.

Weible, M. W. 2nd & Hendry, I. A. 2004. What is the importance of multivesicular bodies in retrograde axonal transport *in vivo*? *J. Neurobiol*. **58**, 230–243.

Yano, H. & Chao, M. V. 2004. Mechanisms of neurotrophin receptor vesicular transport? *J. Neurobiol*. **58**, 244–257.